OCTOBER 1981 LRP 195/81

ALFVEN WAVE COUPLING EXPERIMENTS ON THE TCA TOKAMAK

A. de Chambrier, A.D. Cheetham, A. Heym, F. Hofmann,
B. Joye, R. Keller, A. Lietti, J.B. Lister,
and A. Pochelon

ALFVEN WAVE COUPLING EXPERIMENTS ON THE TCA TOKAMAK

A. de CHAMBRIER, A.D. CHEETHAM*, A. HEYM, F. HOFMANN, B. JOYE,
R. KELLER, A. LIETTI, J.B. LISTER and A. POCHELON.

Centre de Recherches en Physique des Plasmas,
Association Euratom - Confédération Suisse,
Ecole Polytechnique Fédérale de Lausanne,
CH-1007 Lausanne, Switzerland

*present address: Australian National University, Canberra

ABSTRACT

Low power RF absorption experiments have been carried out on the TCA Tokamak using a complete toroidal antenna structure, with ranges of frequency and wavelength such that the shear Alfvén wave can be excited. The general features of the Alfvén absorption are in agreement with predictions.

Excitation of narrow resonance structures with $\Delta\omega/\omega<5\%$ has been observed. These resonances are attributed to low n-number kink modes close to the threshold of the Alfvén continuum at the plasma centre. They are observed for mode helicity of the same sign as that of the magnetic field.

1.INTRODUCTION

The TCA Tokamak experiment was conceived to study the excitation of Alfvén waves as a useful method of plasma heating. Considerable theoretical effort has been devoted to studies of Alfvén Wave Heating using a purely ideal MHD approach (TATARONIS and GROSSMAN, 1973; HASEGAWA and CHEN, 1974; KELLER, 1976; APPERT et al., 1980a, 1980b) and using a kinetic approach (HASEGAWA and CHEN, 1975; PURI, 1980; STIX, 1980; ROSS, CHEN and MAHAJAN, 1981). Heating experiments have so far been carried out mainly in stellarators by DEMIRKHANOV et al. (1976), DIKIJ et al. (1976), GOLOVATO et al. (1976) and OBIKI et al. (1977 and 1978), but also in a theta-pinch by KELLER and POCHELON (1978). An overall review is given by SHOHET (1978).

The present work differs from previous work in several aspects. The antenna structure is discrete, rather than the usual helical antennae. The antenna currents are poloidal resulting in a coupling between antennae and plasma which can be described purely in terms of a local pressure modulation, and which can be therefore treated by ideal MHD. The antenna structure is toroidally complete, and the applied modes can be varied.

This paper describes the study of low power absorption from our antenna structure, carried out prior to heating studies which are now being started (BUGMANN et al., 1981). The total power delivered to the plasma did not exceed a few hundred watts. We give a brief description of the essential theory and of the experiment. The general parametric

dependence of the antenna loading is then discussed, followed by a description of the detailed structure of the loading including peaks of enhanced absorption. Finally, the possibilities of also exploiting these relatively narrow structures for heating or diagnostic purposes are mentioned.

2. THEORY

The shear Alfvén wave frequency given by

$$\omega^2 = \frac{1}{\mu_0 \rho} \left(k B_\phi + m \frac{B_\theta}{r} \right)^2 \qquad (1)$$

is a continuum in a tokamak plasma, due to the radial dependence of mass density ρ and poloidal field B_θ, between a minimum frequency at or near the plasma centre (the threshold frequency) and a maximum frequency at the plasma edge. Toroidal geometry reduces the k-spectrum to a set of n-modes ($k = n/R$) and, fixing the driving frequency, we obtain the Alfvén wave resonance condition

$$\omega^2 = \frac{B_\phi}{\mu_0 \rho(r) R^2} \left(n + \frac{m}{q(r)} \right)^2 \qquad (2)$$

which defines a set of resonant surfaces into which energy can be pumped. An analytic treatment of this problem using a simplified set of ideal MHD equations was originally carried out by KELLER (1976) and KELLER, GRUBER, TROYON (1978) to dimension the TCA experiment. Subsequent detailed numerical solutions of the complete set of equations, obtained by APPERT et al. (1980a, 1980b, 1981), have shown the earlier results to be pessimistic and have demonstrated a good

coupling to the resonant layer, even when this is placed near the plasma centre.

3. THE EXPERIMENT

The TCA tokamak has already been described in detail by CHEETHAM et al. (1980a, 1980b).

The main operating parameters are summarized as:

$R,a = 0.61, 0.17$ m

$B\phi = 5.9 - 15.1$ kG

$q(a) = 18 - 2.2$

$I_p < 135$ kA

$n_e(0) < 9.6 \times 10^{19}$ m^{-3}, H_2 and D_2

The RF antenna structure is illustrated in Fig. 1 and comprises eight separate antenna groups sited above and below the plasma at four equally spaced toroidal locations. Each group consists of 3 separate antenna plates of stainless steel construction, shielded only at the sides by vertical screens, and floating electrically with respect to the torus. The antennae are located 3 cm behind the limiter radius.

Each group is fed separately with its phase determined by its external circuitry. If all antennae are fed in phase they produce an N = 4 configuration which excites modes with n = 0,4,8 etc. Inverting the phase of two antennae produces either N = 1 (exciting all odd-n modes) or N = 2 (exciting modes with n = 2,6,8 etc). The large width of the antennae strongly reduces the coupling to modes with high n-numbers. The RF generator can provide a frequency range of 2-5.5 MHz,

and the complete RF power system has been described in detail by LIETTI et al. (1981).

The measurements of antenna loading were performed using two methods. Firstly, the phase variations of the antenna current with respect to the applied voltage, and secondly, the voltage droop across an extra series resistance were measured. The two methods gave reasonable agreement and the voltage droop was subsequently adopted for reason of its simplicity. The time dependence of some plasma parameters during a typical tokamak shot is shown in Fig. 2, illustrating the technique used to explore the loading. The small antenna current was present throughout the plasma duration and the density was ramped during the shot while keeping the current as constant as possible. In this way the location of the resonant surfaces could be swept continuously, allowing a high resolution measurement of the resulting variation in loading.

4. GENERAL SCALING

We can rearrange the resonance condition, writing the mass density $\rho(r) = m_i \langle A \rangle n_e(r)$, as

$$X \equiv \frac{f^2(MHz)\langle A\rangle n_e(0)\,(10^{19}m^{-3})}{B_\phi^2(T)} = 3.2\,\frac{n_e(0)}{n_e(r)}\left(n+\frac{m}{q(r)}\right)^2 ; \quad f=\frac{\omega}{2\pi}$$

separating the geometrical factors due to current and density profiles from the externally controlled parameters. For a given mode (n,m) the value of X defines the position of the resonant surface. It can be shown that when X is held constant, the antenna loading is only a function of the driving frequency, being in fact proportional to it;

the existance of the kink mode modifies this simple proportionality. Thus, the work done by the antenna current per cycle is only a function of the geometrical parameters and the mode numbers.

A first experiment was carried out with one pair of antenna groups active in the M = 1 configuration, which excites a mixture of modes including all n and odd m. The antenna loading was measured, neglecting fine structure variations, over a wide range of plasma parameters ($n_e(0)$ = 0.6-6 x $10^{19}m^{-3}$, $B\phi$ = 7.8 - 15.1 kG, f = 2.7 and 5.0 MHz, q(a)~4, D_2). The antenna loading (expressed as the equivalent series resistance per antenna group) is shown in Fig. 3(a) as a function of line-averaged electron density $\overline{n}_e$, and the normalised loading (mΩ/MHz) is shown as a function of X in Fig. 3(b).

The reduction of the loading to a single parametric dependence is well demonstrated. The constancy of these loading measurements with respect to variations of antenna current was found to be good over the factor of 20 in absorbed power studied. The experimental form of the frequency dependence of the loading curve is close to the curve obtained if the power is proportional only to the square of the antenna volts, shown in Fig. 3(b) as a dotted line. If a large number of (n,m) modes is excited, the antenna voltage is independent of the driving frequency for a fixed value of the power absorbed by the plasma.

5. DETAILS OF ABSORPTION

Fig. 4(a) shows a typical antenna voltage trace in detail as a function of time, implicitly as a function of density during the middle of the pulse, and Fig. 4(b) shows the value of antenna loading

deduced from this figure. We see that there is a considerable structure in this case, for which the excitation configuration was N = 2 (exciting n = 2,6...), M = 1 (exciting m = ±1, ±3 ...). The dominant feature is a large peak with the absorption greater on the low density side than on the high density side.

The peaks in absorption are found to occur at values of plasma parameters for which an Alfvén continuum defined by equation (2) is at its threshold near the plasma centre. This occurs for fixed values of the X-parameter calculated from simple models of the density and current profiles, such profiles not being experimentally measured. By varying the plasma parameters over as wide a range as possible (X = 8-180) we have been able experimentally to identify the peaks corresponding to n = 1,2,3,4,5 with an indication of the presence of n = 6, all being m = +1 modes as defined in equation (2). They correspond to modes with the same sign of helicity as the total magnetic field. No peaks have been detected for the m = -1 modes,although their corresponding thresholds have been covered by the experiment.

Fig. 5 shows the changes in the antenna loading as the excitation configuration was altered. We found that the N = 2 configuration produced the same large peak and in addition a second smaller peak at higher density. The N = 1 (n = 1,3,5 ...) configuration produced peaks at similar densities but the second is now the bigger. The N = 4 (n = 0,4, 8 ...) configuration shows only a small sign of these peaks. On changing from N = 2, M = 1 to N = 2, M = 2 we observed a reduction in absorption by a factor of 2. The two peaks correspond to n = 2 and n = 3 respectively. The reduction in absorption for M = 2 has been generally predicted.

The change in absorption for a density greater than at the peak corresponds to the increased loading due to the presence of a new (n,m) continuum at the centre of the plasma. The abruptness of this change in absorption is in agreement with the numerical results previously obtained by APPERT et al. (1980a), but the subsequent behaviour is different from that predicted by their 1-D numerical ideal MHD model. The identification of the steps in absorption for modes m = +1 is aided by the presence of the narow peaks, but so far definite evidence of similar steps for the m = -1 thresholds has been found only for n = 2.

The existence of the narrow absorption peaks is attributed to the presence of the kink-mode close to the threshold of the Alfvén continuum. It has already been shown by POCHELON et al. (1975) that the radial profile of the kink-mode becomes more and more peaked as it approaches the Alfvén continuum. The behaviour of the kink as it would cross into the continuum is complex, but it has been seen in the same work that the kink can be repelled by the Alfvén continuum and remain outside it as a discrete mode. This effect is being studied in detail in ideal MHD calculations by APPERT et al. (1981) in support of this experiment and has been shown to be extremely sensitive to the density and safety-factor profiles. These calculations have also shown absorption peaks due to the kink mode only for m = +1 modes. Previous work by ROSS et al. (1981) proposed that such peak enhancement is produced by kinetic effects, although even a greatly simplified analytic MHD model has been able to reproduce the peak structures.

The behaviour of the resonance peaks was investigated in greater detail. The value of line-averaged density at which they occur depends on the plasma current, the resonant density increasing as the safety-factor q(a) is reduced for all peaks observed. The width and density of one such peak (n = 2, m = 1) are shown as a function of current in Fig. 6. Also plotted is the square root of the resonant density, the location of the resonance being given approximately by

$$f \propto \left(\langle A \rangle n_e(0) \right)^{1/2} \sim B_\phi \left(n + \frac{m}{q(0)} \right)$$

which is shown as a dotted line in the figure assuming parabolic q and density profiles. We see that the slope is in good agreement with the data. At high current, however, the dependence is reduced, which may be explained in terms of the commonly observed flattening of the q profile as q(a) is reduced towards 3. At low current the dependence is increased, explained by a probable peaking of the density profile.

Since the loading represents a measurement of power, the coupling coefficient (expressed in terms of a force) is proportional to the width of the peak ($\Delta\omega/\omega$) times the square root of its height. This coupling is shown in Fig. 6, in which we see that at high values of q(a) it increases linearly with increasing current, as predicted for the continuum in the numerical calculations of APPERT et al. (1980a), but that as q(a) approaches 3 the coupling saturates. This can similarly be explained in terms of a flattening of the q profile at lower values of q(a), which has numerically been shown to be an important factor in the coupling.

The peaks are not always visible when crossing an Alfvén threshold and they are in such cases replaced by the step in absorption

which is also seen when they are present. In general, this absence occurs at lower values of field and the higher value of frequency. Since $\bar{n}_e$ (peak)$\sim(B\phi/\omega)^2$ this corresponds to the lowest densities, and the highest values of ω/ω_{ci}. Changing the working gas from deuterium to hydrogen failed to cause the peaks to reappear, suggesting that ω/ω_{ci} is not the critical factor. The change in profiles at low density could explain their absence. On changing from deuterium to hydrogen in the presence of a peak we observed a change of its line-averaged density of less than a factor of 2. This comes from the fact that the average ion mass is $\sim$1.3 when working in hydrogen and $\sim$2 when working in deuterium, calculated from estimates of impurity content giving $Z_{eff} \sim 3$, with the light impurities being dominant.

The final experimental observation concerning the resonance peaks was their modulation in amplitude synchronously both with island rotation at frequencies of $\sim$10-15 kHz, as seen on the poloidal field modulation and soft X-ray emission modulation, and with the sawteeth seen on the soft X-ray emission signals. The absorption changes can be explained by the modulation of the antenna-plasma distance due to island rotation, or by a direct modification of the MHD coupling produced by the slight triangular or elliptic deformation of the surfaces as suggested by APPERT et al. (1981).

Two interesting points arise in connection with the absorption peaks. Firstly, the evidence of the enhanced absorbtion by the kink modes suggests the experimental possibility of an efficient core heating and current-drive, since it is known that for these modes the radial profile of the amplitude is extremely peaked at the centre.

Secondly, the dependence of their location on the quantity $(n+m/q(0))\rho(0)^{-1/2}$ allows their use as a diagnostic method. This has been proposed by JOYE et al. (1981) for measuring the values of mass density $\rho(0)$ and safety-factor $q(0)$ on axis, both of which are indirectly derived in present Tokamaks. The antenna structure required inside the vacuum vessel is extremely simple, compatible with some existing ICRH antennae and only simple external circuitry is required. The validity of the technique has been demonstrated by the changes in the electron density at resonance as the working gas was varied.

6. CONCLUSION

We have experimentally demonstrated that the main absorption from antennae working in the Alfvén range of frequencies scales with plasma parameters in the way predicted and that the Alfvén modes excited are defined by a fully toroidal but discrete antenna structure. The behaviour of the antenna loading is in agreement with purely MHD theoretical predictions. In addition, peaks of enhanced absorption have been seen near the threshold of the Alfvén continuum for $n = 1\text{-}5$, $m = 1$, explained in terms of the the kink mode. Their use for heating, current-drive and as a diagnostic is mentioned.

ACKNOWLEDGEMENT

We wish to thank K. Appert, B. Balet and J. Vaclavik for substantial discussions on the theoretical questions, and P.D. Morgan and F. Troyon for their comments on this paper.

This work was supported by the Swiss National Science Foundation and by Euratom.

REFERENCES

APPERT K., BALET B., GRUBER R., TROYON F. and VACLAVIK J. (1980a) 8th Int. Conf. on Plasma Physics and Contr. Nucl. Fusion Research, Brussels, Vol. II, 43.

APPERT K., BALET B., GRUBER R., TROYON F., TSUNEMATSU T. and VACLAVIK J (1980 b) 2nd Joint Grenoble-Varenna Int. Symp. on Heating in Toroidal Plasmas, Como, paper 7.

APPERT K., BALET B., GRUBER R., TROYON F., TSUNEMATSU T. and VACLAVIK J. (1981) to be published.

BUGMANN G., de CHAMBRIER A., CHEETHAM A.D., HEYM A., HOFMANN F., JOYE B., KELLER R., LIETTI A., LISTER J.B., POCHELON A., SIMIK A., SIMM W.C., TONINATO J.-L. and TUSZEL A. (1981) 10th European Conf. on Controlled Fusion and Plasma Physics, Moscow.

CHEETHAM A.D., HEYM A., HOFMANN F., HRUSKA K., KELLER R., LIETTI A., LISTER J.B., POCHELON A., RIPPER H., SCHREIBER R. and SIMIK A. (1980 a) Lausanne Report LRP 162/80

CHEETHAM A.D., HEYM A., HOFMANN F., HRUSKA K., KELLER R., LIETTI A., LISTER J.B., POCHELON A., RIPPER H., SIMIK A. and TUSZEL A. (1980 b) 11th Symp. on Fusion Technology, Oxford, Vol. 1, 601.

DEMIRKHANOV R.A., KIROV A.G., LOZOVSKIJ S.N., NEKRASOV F.M., ELFIMOV A.G., IL'INSKIJ S.E. and ONISHCHENKO V.V. (1976) 6th Int. Conf. on Plasma Physics and Contr. Fusion Research, Berchtesgarden, Vol. III, 31.

DIKIJ A.G., KALINICHENKO S.S., KUSNETSOV Y.K., KURILKO P.I., LYSOJVAN A.I., PASHNEV V.K., TARASENKO V.F., SUPRUNENKO V.A., TOLOK V.T. and SHVETS O.M. (1976) 6th Int. Conf. on Plasma Physics and Contr. Fusion Research, Berchtesgaden, Vol. II, 129.

GOLOVATO S.N., SHOHET J.L. and TATARONIS J.A. (1976) Phys. Rev. Lett. 39, 1272.

HASEGAWA A. and CHEN L. (1974) Phys. Rev. Lett. 32, 454.

HASEGAWA A. and CHEN L. (1975) Phys. Rev. Lett. 35, 370.

JOYE B., LIETTI A., LISTER J.B. and POCHELON A. (1981) Lausanne Report LRP 196/81

KELLER R. (1976) Lausanne Report LRP 104/76

KELLER R., GRUBER R. and TROYON F. (1978) Joint Varenna-Grenoble Int. Symp. on Heating in Toroidal Plasmas, Grenoble, Vol. 2, 195.

KELLER R. and POCHELON A. (1978) Nucl. Fusion 18, 1051.

LIETTI A., BUGMANN G., de CHAMBRIER A., HEYM A., HOFMANN F., JOYE B., KELLER R., LISTER J.B., POCHELON A., SIMIK A., SIMM W.C., TONINATO J.-L. and TUSZEL A. (1981) 9th Symposium on Engineering Problems of Fusion Research, Chicago.

OBIKI T., MUTOH T., ADACHI S., SASAKI A., IIYOSHI A. and UO K. (1977) Phys. Rev. Lett. 39, 812.

OBIKI T., MUTOH T., KINOSHITA S., SATO M., IIYOSHI A. and UO K. (1978) Joint Varenna-Grenoble Int. Symp. on Heating in Toroidal Plasmas, Grenoble Vol. 1, 109.

POCHELON A., KELLER R., TROYON F., and GRUBER R. (1975) Proc. of 7th Europ. Conf. on Contr. Fusion and Plasma Physics, Lausanne, Vol I, 157

PURI S. (1980) 2nd Joint Grenoble-Varenna Int. Symp. on Heating in Toroidal Plasma, Como.

ROSS D.W., CHEN G.L. and MAHADJAN S.M. (1981) Fourth Topical Conf. on RF Heating in Plasma, Austin, Texas, paper B 14.

SHOHET J.L. (1978) Comments Plasma Phys. Cont. Fusion, 4, 37

STIX Th. H. (1981) 2nd Joint Grenoble-Varenna Int. Symp. on Heating in Toroidal Plasmas, Como, paper 6.

TATARONIS J.A. and GROSSMANN W. (1973) Z.Physics, 261, 203 and 217

FIGURE CAPTIONS

Fig. 1 Alfvén wave antenna structure used in the TCA Tokamak.

Fig. 2 Typical Tokamak shot (B_ϕ = 11.6 kG, D_2, N = 2, M = 1, f = 5.0 MHz) showing plasma current, loop volts, line-averaged electron density and antenna voltage.

Fig. 3 Single Antenna Loading (a) Loading vs. electron density (b) Reduced loading vs. scaling parameter X.

Fig. 4 Antenna behaviour as a function of time (a) Antenna voltage (b) Deduced loading resistance (B_ϕ = 15.1 kG, f = 2.67 MHz, N = 2, M = 1)

Fig. 5 Effect of varying the excitation configuration.

Fig. 6 Current dependence of the peaks (a) FWHM and coupling factor (b) Density and its square root.

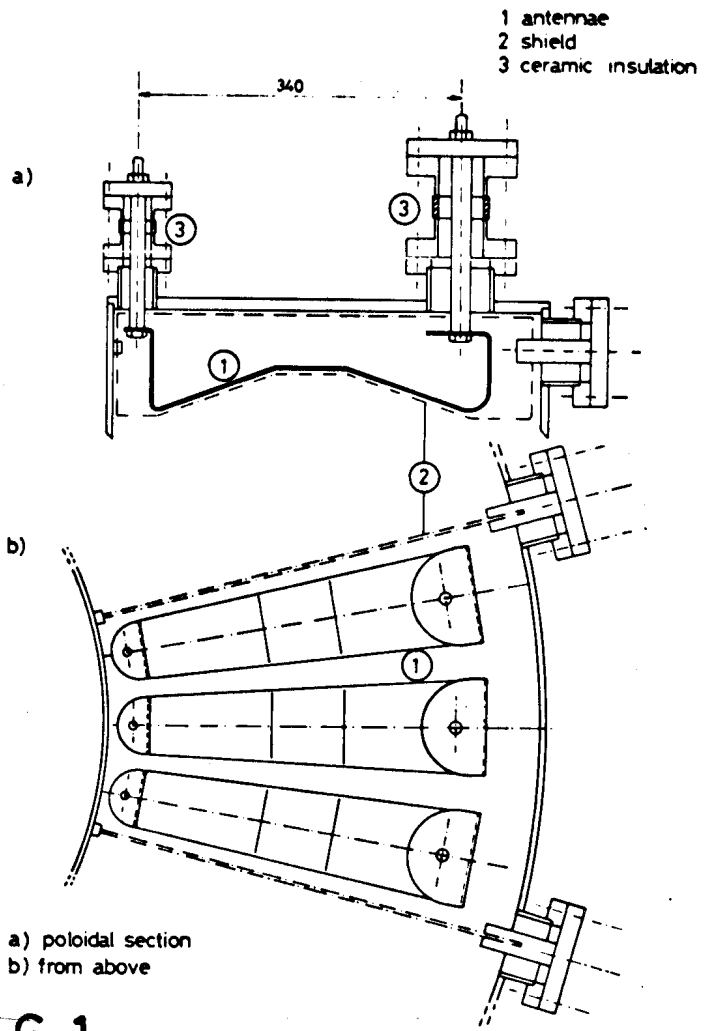
1 antennae
2 shield
3 ceramic insulation
340
a)
b)
a) poloidal section
b) from above

FIG.1

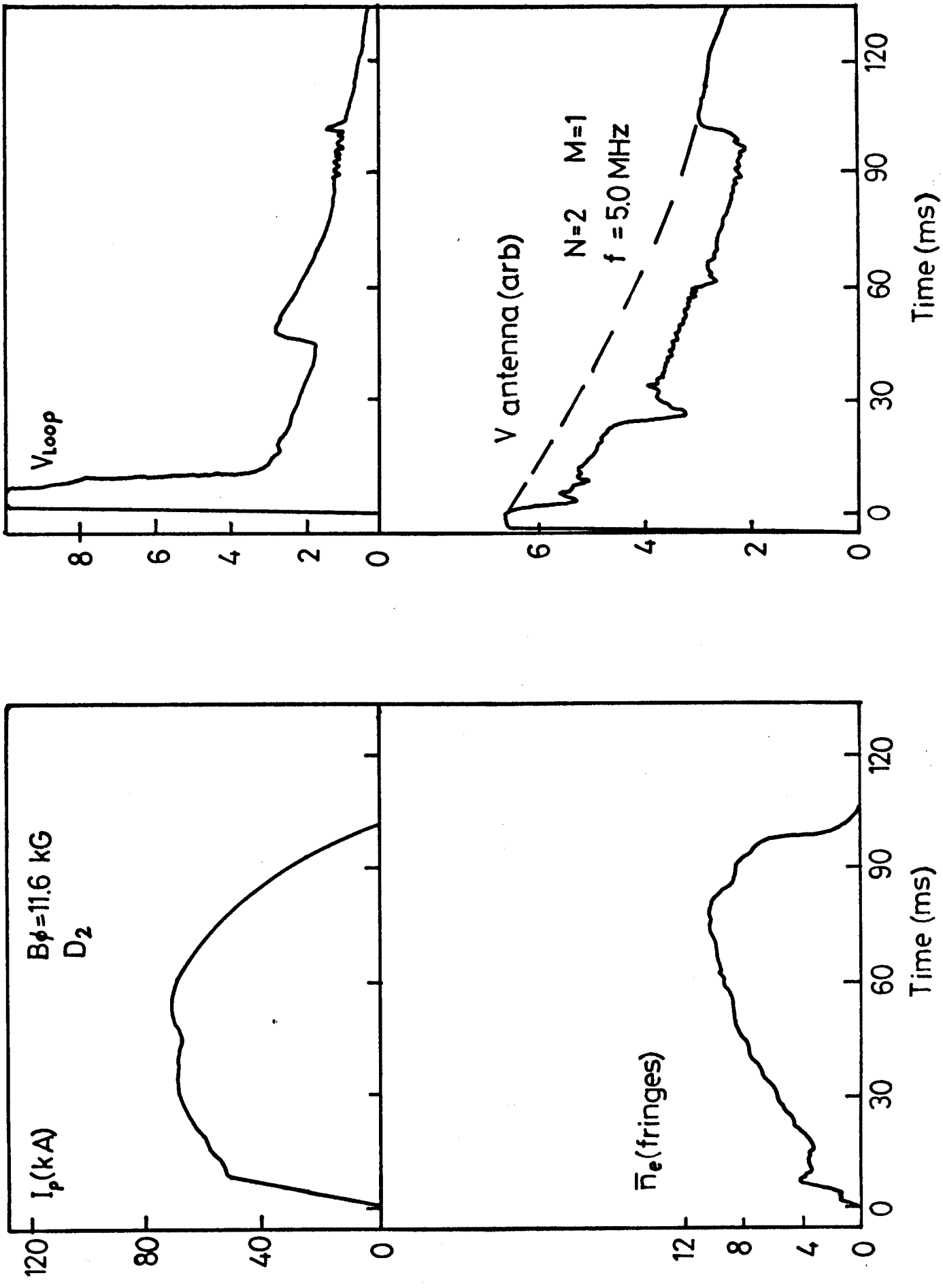
I_p(kA)
Bϕ=11.6 kG
D_2
120
80
40
0
$\bar{n}_e$(fringes)
12
8
4
0
0
30
60
90
120
Time (ms)
V_{loop}
8
6
4
2
0
V antenna (arb)
N=2 M=1
f = 5.0 MHz
6
4
2
0
0
30
60
90
120
Time (ms)

FIG. 2

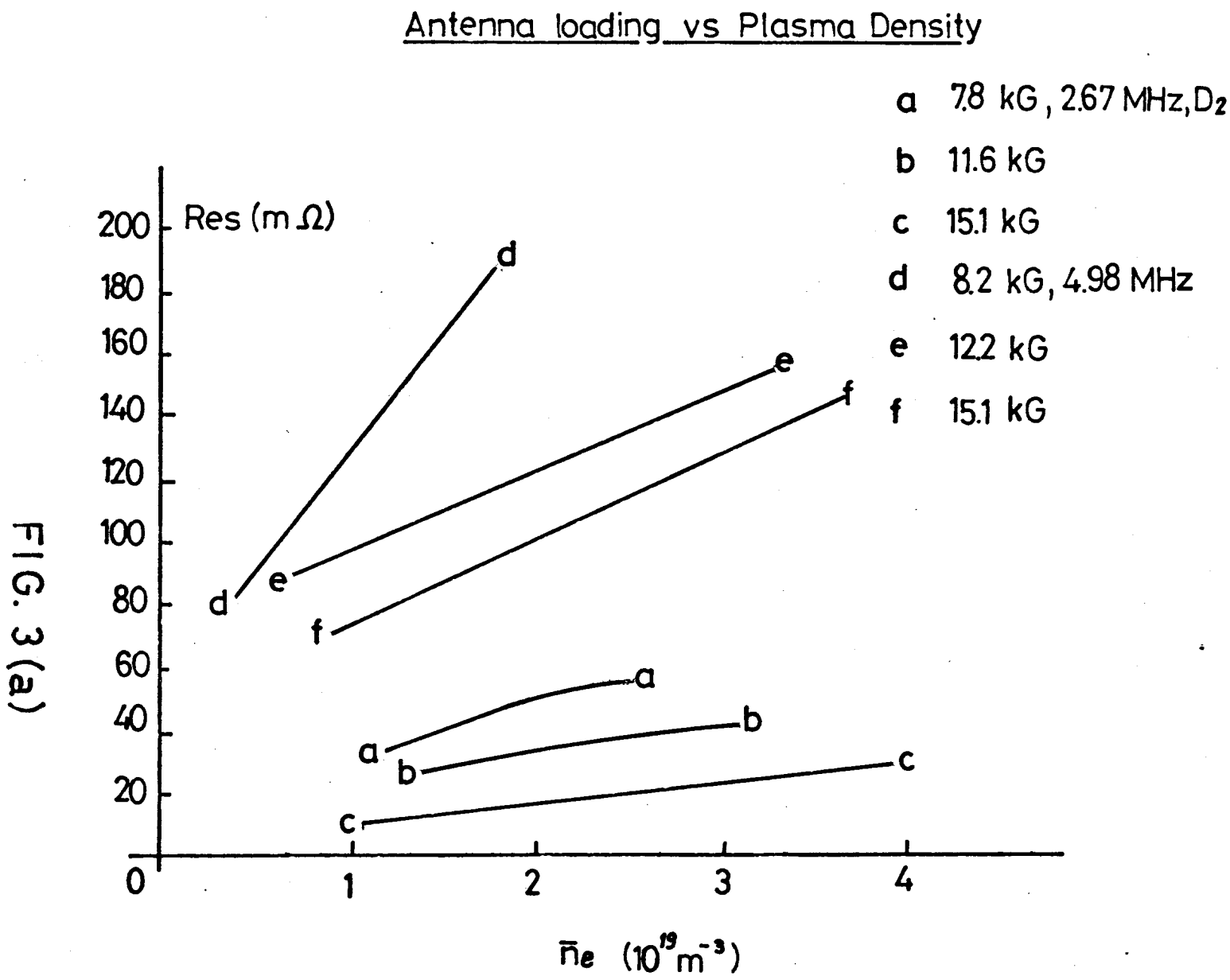
Antenna loading vs Plasma Density
a 7.8 kG, 2.67 MHz, D2
b 11.6 kG
c 15.1 kG
d 8.2 kG, 4.98 MHz
e 12.2 kG
f 15.1 kG
Res (m Ω)
200
180
160
140
120
100
80
60
40
20
0
1
2
3
4
ñe (10^19 m^-3)

FIG. 3(a)

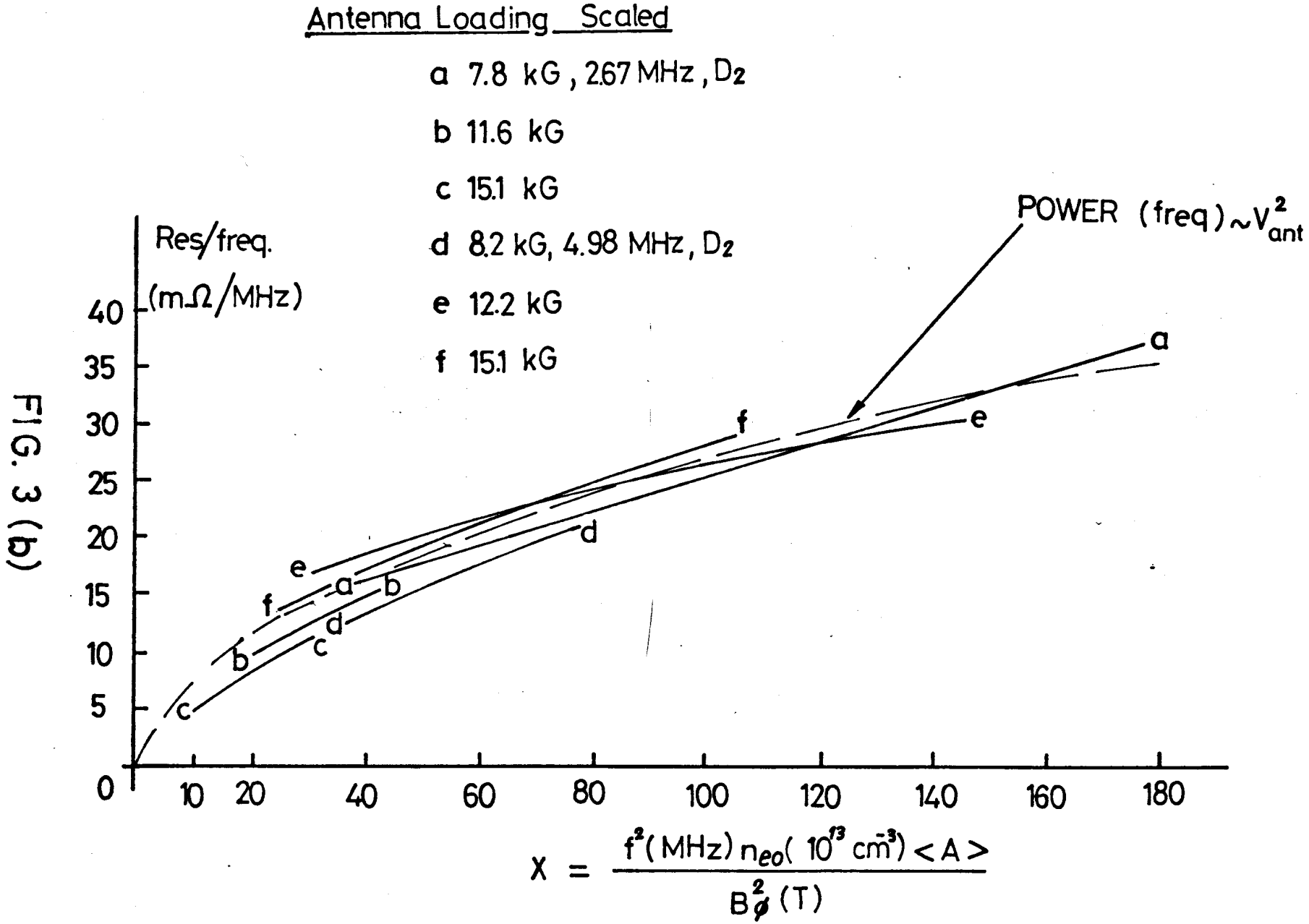
Antenna Loading Scaled
a 7.8 kG, 2.67 MHz, D2
b 11.6 kG
c 15.1 kG
d 8.2 kG, 4.98 MHz, D2
e 12.2 kG
f 15.1 kG
POWER (freq) ~ V²ant
Res/freq.
(mΩ/MHz)
40
35
30
25
20
15
10
5
0
10
20
40
60
80
100
120
140
160
180
X = f²(MHz) neo(10¹³ cm⁻³) <A> / B²φ (T)

FIG. 3 (b)

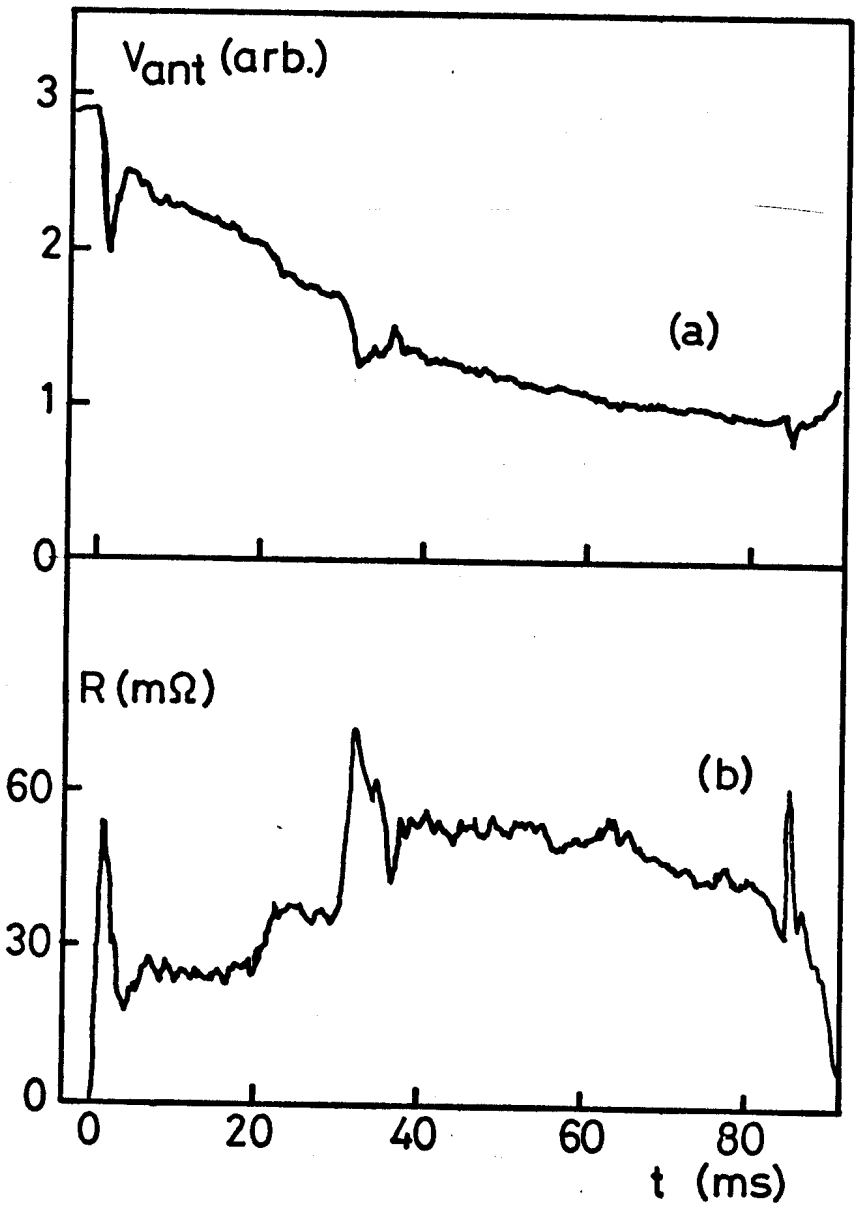

FIG. 4

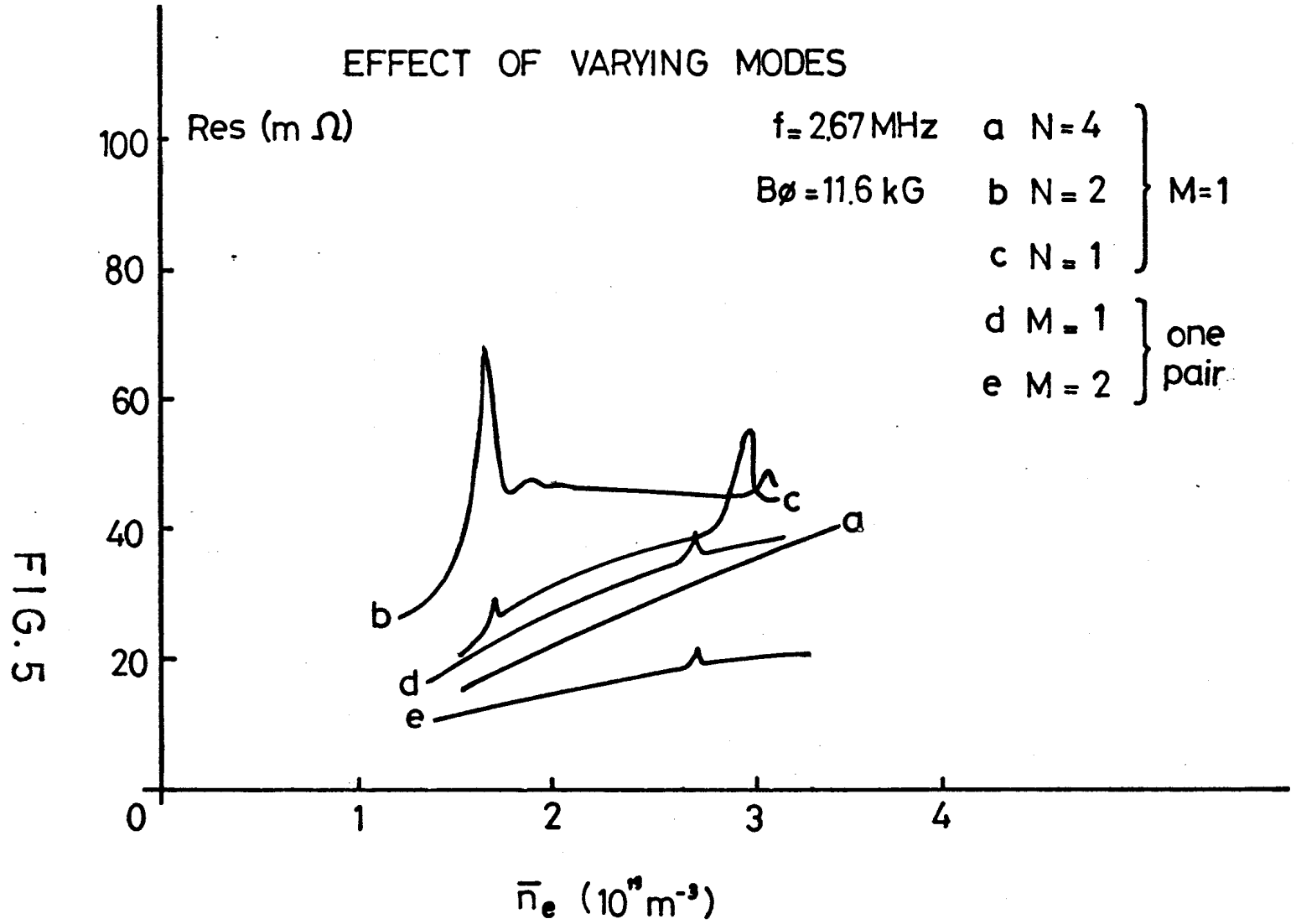
EFFECT OF VARYING MODES
Res (m Ω)
f = 2.67 MHz
Bø = 11.6 kG
a N = 4
b N = 2
c N = 1
M=1
d M = 1
e M = 2
one pair
100
80
60
40
20
0
1
2
3
4
a
b
c
d
e
$\bar{n}_e$ (10^{19} m^{-3})

FIG. 5

FIG. 6

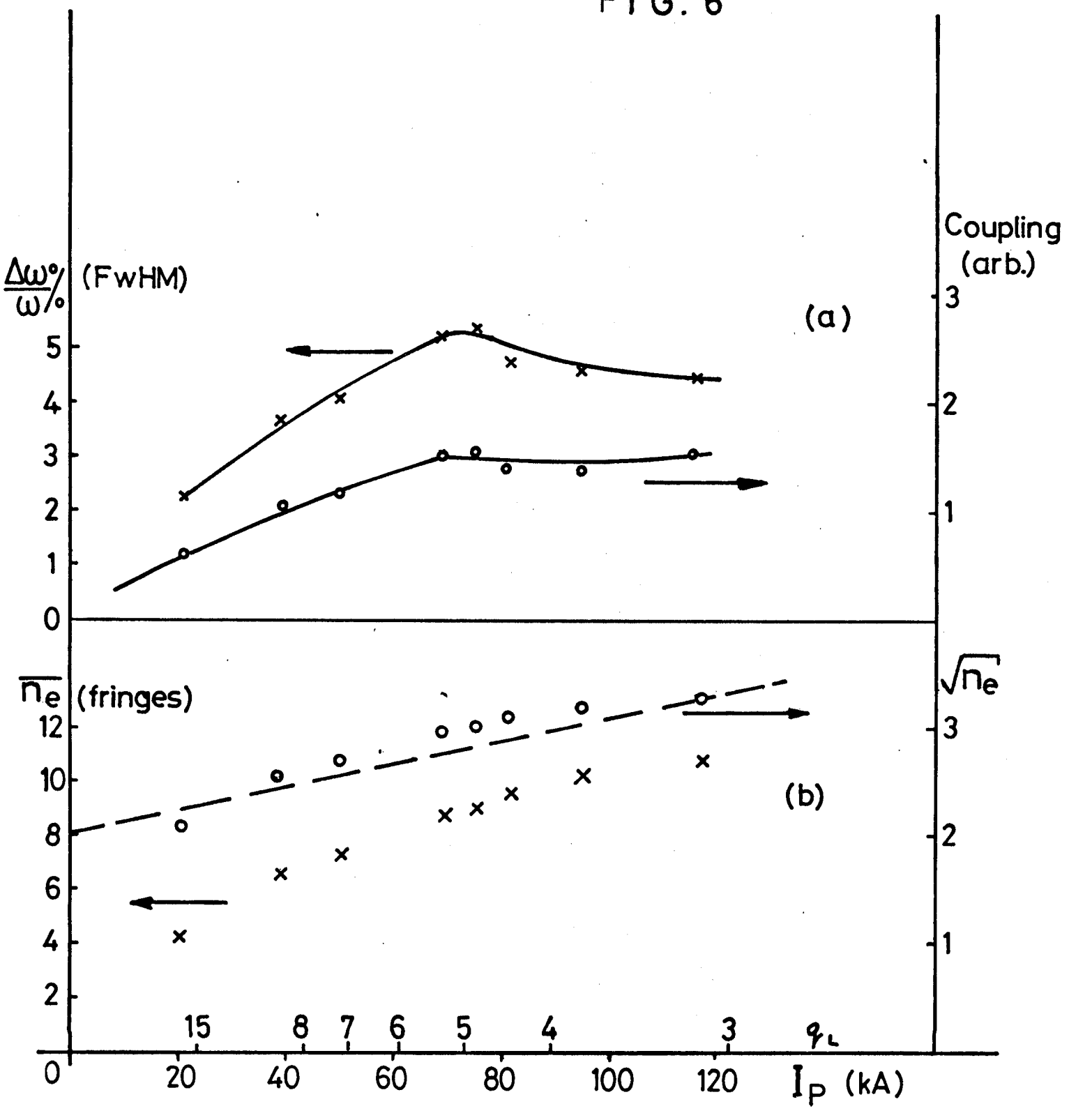
Δω%/ω% (FwHM)
(a)
Coupling (arb.)
0
1
2
3
4
5
n̄e (fringes)
(b)
√n̄e
6
8
10
12
15
8
7
6
5
4
3
qL
0
20
40
60
80
100
120
IP (kA)